

The Redshift Evolution of the Mass Function of Cold Gas in Hierarchical Galaxy Formation Models

C. Power^{*1,2}, C. M. Baugh³ & C. G. Lacey³

¹ *Department of Physics & Astronomy, University of Leicester, Leicester LE1 7RH, United Kingdom*

² *Centre for Astrophysics and Supercomputing, Swinburne University of Technology, PO Box 218, Hawthorn, 3122, Victoria, Australia*

³ *Institute for Computational Cosmology, University of Durham, South Road, Durham DH1 3LE, United Kingdom*

ABSTRACT

Accurately predicting how the cosmic abundance of neutral hydrogen evolves with redshift is a challenging problem facing modellers of galaxy formation. We investigate the predictions of four currently favoured semi-analytical galaxy formation models for the mass function of cold neutral gas (atomic and molecular) in galaxies as a function of redshift, and we use these predictions to construct number counts for the next generation of all-sky neutral atomic hydrogen (HI) surveys. Despite the different implementations of the physical ingredients of galaxy formation, we find that the model predictions are broadly consistent with one another; the key differences reflect how the models treat AGN feedback and how the timescale for star formation evolves with redshift. The models produce mass functions of cold gas in galaxies that are generally in good agreement with HI surveys at $z=0$. Interestingly we find that these mass functions do not evolve significantly with redshift. Adopting a simple conversion factor for cold gas mass to HI mass, we derive mass functions of HI in galaxies from the predicted mass functions of cold gas, which we use to predict the number counts of sources likely to be detected by HI surveys on next generation radio telescopes such as the Square Kilometre Array and its path-finders. We find the number counts peak at $\sim 4 \times 10^4/2 \times 10^5/5 \times 10^5$ galaxies per square degree at $z \sim 0.4/0.8/1.4$ for a year long HI survey on a 1%/10%/100% SKA. We also examine how the typical angular sizes of galaxies vary with redshift. These decline strongly with increasing redshift at $z \lesssim 0.5$ and more gently at $z \gtrsim 0.5$; the median angular size varies between $5''$ and $10''$ at $z=0.1$, $0.5''$ and $3''$ at $z=1$ and $0.2''$ and $1''$ at $z=3$ for galaxies with HI masses in excess of $10^9 h^{-1} M_\odot$, depending on the precise model. Taken together, these results make clear that forthcoming HI surveys will provide important and powerful tests of theoretical galaxy formation models.

Key words: cosmology: theory – galaxies: formation – radio lines: galaxies

1 INTRODUCTION

Neutral gas, predominantly atomic hydrogen (HI) along with molecular hydrogen (H_2) and helium (He), plays a fundamental role in galaxy formation, principally as the raw material from which stars are made. At any given time the fraction of a galaxy's mass that is in the form of HI will be determined by the competing rates at which it is depleted (by, for example, star formation, photo-ionisation and expulsion via winds) and replenished (by, for example, recombination and accretion from the galaxy's surroundings). These processes are integral to any theory of galaxy formation and so we expect that understanding how the HI properties of

galaxies vary with redshift and environment will provide us with important insights into how galaxies form.

Our knowledge of HI in galaxies derives from radio observations of the rest-frame 21-cm emission line, which allows us to measure the density, temperature and velocity distribution of HI along our line of sight. Thanks to surveys such as HIPASS (HI Parkes All-Sky Survey; see Meyer et al. 2004) and more recently ALFALFA (Arecibo Legacy Fast ALFA Survey; see Giovanelli et al. 2005), we have a good understanding of the HI properties of galaxies in the low-redshift Universe, at $z \lesssim 0.05$. For example, HIPASS has revealed that most HI is associated with galaxies and that the galaxy population detected in 21-cm emission is essentially the same as that seen at optical and infrared wavelengths but weighted towards gas-rich systems, which tend to be

* chris.power@astro.le.ac.uk

late-type (Meyer et al. 2004). Furthermore, HIPASS data have allowed accurate measurement of the local HI mass function of galaxies (the number density of galaxies with a given HI mass per unit comoving volume) and Ω_{HI} (the global HI mass density in units of the present-day critical density $\rho_{\text{crit}} = 3H_0^2/8\pi G$). Zwaan et al. (2005) found that the local HI mass function is well described by a Schechter function and they estimated the local cosmic HI mass density to be $\Omega_{\text{HI}} = 3.5 \pm 0.4 \pm 0.4 \times 10^{-4} h_{75}^{-1}$ (with random and systematic uncertainties at the 68% confidence limit), assuming a dimensionless Hubble parameter of $h_{75}=0.75$. This is approximately $1/10^{\text{th}}$ the value of cosmic stellar mass density Ω_{ast} at $z=0$ (cf. Cole et al. 2001).

In contrast, we know comparatively little about HI in galaxies at higher redshifts (i.e. $z \gtrsim 0.05$). This is because detecting the rest frame 21-cm emission from individual galaxies has required too great a sensitivity for reasonable observing times¹. There are estimates of Ω_{HI} at high redshifts ($z \gtrsim 1.5$) but these have been deduced from QSO absorption-line systems and imply that $\Omega_{\text{HI}} \simeq 10^{-3}$ (e.g. Péroux et al. 2003; Prochaska et al. 2005; Rao et al. 2006). However, this situation will change dramatically over the next decade with the emergence of a series of next generation radio telescopes, culminating in the Square Kilometre Array (SKA) that is expected to see first light by about 2020. The SKA will have sufficient sensitivity and angular resolution to map HI in galaxies out to redshifts $z \gtrsim 3$ (see, for example Blake et al. 2004; Braun 2007). On a shorter timescale a variety of SKA path-finders such as ASKAP (the Australian SKA Pathfinder; see Johnston et al. 2008), MeerKAT (the Karoo Array Telescope; see Jonas 2007) and APERTIF (APERture Tile In Focus; see Verheijen et al. 2008) will carry out HI surveys that, in some cases, will probe the properties of galaxies out to $z \sim 1$.

Because we have so little data on HI in galaxies beyond the local Universe, the results of HI surveys on next generation radio telescopes will have a profound impact on our understanding of galaxy formation and evolution. For example, we have compelling evidence that the cosmic star formation rate density has decreased by an order of magnitude since $z \sim 1$ (Madau et al. 1996; Hopkins 2004), yet we know little about how the HI mass in galaxies evolved over the same period. This is precisely the kind of question we can hope to answer with forthcoming HI surveys. For this reason it is both timely and important to take stock of what theoretical galaxy formation models tell us about how quantities such as Ω_{HI} and the HI mass function vary with redshift and environment. Not only can such predictions help us to interpret the physical significance of observational data, they can also provide important input into the design of new radio telescopes.

The primary aim of this paper is to explore the predictions of currently favoured *semi-analytical* galaxy formation models (cf. Cole et al. 2000; Baugh 2006) for the

properties of cold gas in galaxies as a function of redshift in a Λ Cold Dark Matter (Λ CDM) universe. In particular we investigate how the cold gas mass function and Ω_{cold} vary with redshift. We also convert the predicted cold gas masses to HI masses and we use the resulting HI mass functions, along with predictions for the radii and rotation speeds of galactic discs, to predict the number counts of sources one might expect to recover from HI surveys on a radio telescope with a collecting area of 1%/10%/100% the full SKA. The secondary aim of this paper is to compare and contrast the predictions of four distinct galaxy formation models from the Durham and Munich groups. These models incorporate different treatments of the same physical processes and in some cases invoke distinct physical processes (for example, AGN heating versus supernova-driven super-winds) and so it is instructive to assess the robustness of the basic predictions and to examine whether or not these predictions are consistent between models. This addresses the criticism that semi-analytical galaxy formation models lack transparency and uncertainty as to which predictions are robust and which are sensitive to modest changes in the model parameters. This work complements in a very natural way the recent study of Obreschkow et al. (2009a).

The layout of the paper is as follows. In § 2 we present an overview of the four galaxy formation models we use in this study. In § 3 we examine the basic predictions of these models for the evolution of the mass function and global mass density of cold gas between $0 \lesssim z \lesssim 2$, and we determine the relationship between cold gas mass and the circular velocities and scale radii of discs. Based on these predictions, in § 4 we determine what the implications are for the number counts of HI sources in future HI surveys on next generation radio telescopes. Finally, in § 5 we summarise our results and discuss how future HI surveys will provide a powerful test of theoretical models of galaxy formation.

2 GALAXY FORMATION MODELS

The evolution of the global cold gas density in the Universe and the cold gas content of galaxies depend upon the interplay between a number of processes:

- (i) the rate at which gas cools radiatively within dark matter haloes;
- (ii) the rate at which cold gas is accreted in galaxy mergers;
- (iii) the rate at which cold gas is consumed in star formation;
- (iv) the rate at which gas is reheated or expelled from galaxies by sources of feedback (e.g. photoionisation, stellar winds, supernovae, AGN heating, etc.).

Semi-analytical modelling provides us with the means to study the balance between these phenomena in the context of a universe in which structure in the dark matter grows hierarchically (for a recent review, see Baugh 2006). The models refer to cold gas as gas that has cooled radiatively from a hot phase to below $10^4 K$ and is available for star formation. The cold gas mass is predominately made up of neutral atomic hydrogen (HI), along with molecular hydrogen and helium.

¹ Although in a handful of cases it has been possible to use a stacking technique to measure rest frame 21-cm emission by co-adding the signal from multiple galaxies using their observed optical positions and redshifts; see Zwaan (2000), Chengalur et al. (2001) and Lah et al. (2007, 2009).

Here we consider four different semi-analytical galaxy formation models from the Durham and Munich groups. Although the models follow the same basic philosophy, the implementations of various processes differ substantially between the two groups. We also consider Durham models with different physical ingredients. To remove one possible source of difference between the models, all the models discussed here adopt the background cosmology used in the Millennium simulation ($\Omega_M=0.25$, $\Omega_\Lambda=0.75$, $\Omega_b = 0.045$, $\sigma_8=0.9$) and use the halo merger histories extracted from the simulation (Springel et al. 2005).²

We now list the different models considered in this paper, give their designation and a very brief description of the main features of each. The differences between the models are discussed in more detail later on in this section. The first three models are “Durham” models which use the GALFORM code and the fourth model is the current “Munich” semi-analytical model. The model designations are those used in the Millennium Archive³ and in the subsequent plots.

- The Bower et al. (2006) model (hereafter Bower2006a). AGN heating suppresses the formation of bright, massive galaxies by stopping the cooling flow in the host dark matter halo, thereby cutting off the supply of cold gas for star formation. This regulation of the cooling flow results in a sharp break at the bright end of the luminosity function. This model matches the evolution of the stellar mass function inferred from observations (e.g. Fontana et al. 2004; Drory et al. 2005), the number counts and redshift distribution of extremely red objects (Gonzalez-Perez et al. 2008b) and the abundance of luminous red galaxies (Almeida et al. 2008).

- The Font et al. (2008) model (hereafter Font2008a). This extends Bower2006a with a fundamental change to the cooling model. Motivated by the simulations of McCarthy et al. (2008), which track the fate of the hot gas in haloes after their accretion by more massive objects, Font et al. assume that the stripping of hot gas from satellite haloes is not completely efficient, contrary to the traditional recipe used in semi-analytical models. Instead, the satellite halo is assumed to retain some fraction of its hot gas, which is determined by its orbit within the larger halo. This gas can cool directly onto the satellite rather than the central galaxy in the halo. Font2008a gives an improved match to the proportions of red and blue galaxies seen in SDSS groups (Weinmann et al. 2006a,b).

- The Baugh et al. (2005) model (hereafter Baugh2005M). This matches the observed counts and redshifts of sub-mm galaxies and the luminosity function of Lyman-break galaxies, as well as observations of the local galaxy population. In this model, merger-triggered starbursts make a similar contribution to the star formation rate per unit volume at high redshift to that from galactic discs. Starbursts are assumed to have a top-heavy stellar

initial mass function (IMF), which Baugh et al. argue is essential for a hierarchical galaxy formation model to match the sub-mm counts, whilst at the same time reproducing observations of local galaxies. The formation of bright galaxies is regulated by a supernova driven “super-wind”, which expels gas from intermediate mass dark matter haloes (see Benson et al. 2003). In this paper we implement Baugh2005M in the Millennium simulation. The cosmology used in the Millennium is somewhat different to that adopted in the original Baugh et al. model (the former has a matter density of $\Omega_M = 0.25$ whereas the latter used $\Omega_M = 0.3$). To reproduce the predictions of Baugh et al. (2005), we retain the baryon fraction of the original model, setting $\Omega_b = 0.033$. The other galaxy formation parameters have *not* been changed. This model is not available in the Millennium Archive.

- The De Lucia & Blaizot (2007) model (hereafter DeLucia2006a). This also employs AGN-feedback in the “radio-mode” to restrict the formation of bright galaxies at the present day. This model is a development of those introduced by Croton et al. (2006) and De Lucia et al. (2006). This model enjoys many of the same successes as Bower2006a, but, if anything, produces too many stars at high redshift (cf. Kitzbichler & White 2007)

We now highlight some of the areas in which there are either important differences in the implementation of the physics between the models or in which different processes have been adopted. For full descriptions of each model we refer the reader to the original references given above. A comparison of Bower2006a and Baugh2005M was given by Almeida et al. (2007); the differences between Bower2006a and Font2008a are set out in Font et al. (2008).

(1) *Gas cooling: gas density and cooling radius.* The models all assume that gas cools primarily (for the haloes which typically host galaxies) by two-body collisional processes involving neutral or ionised atoms. The cooling rate depends upon the composition (metallicity) and the density of the gas. Gas is assumed to have cooled within some cooling radius, which is defined in different ways in the models. A further timescale which regulates the addition of cold gas into a galactic disc is the free-fall time. The models make different assumptions about the density profile of the gas and the cooling radius: (i) DeLucia2006a assume that the gas has a singular isothermal profile (see Croton et al. 2006). The cooling radius is defined as the radius at which the cooling time is equal to the dynamical time of the halo. (ii) Bower2006a and Font2008a assume that the hot gas density profile is an isothermal with a constant density core. The core radius is fixed and scales with the virial radius of the halo. The cooling radius propagates outwards as a function of time, reaching a maximum at the radius where the cooling time is equal to the lifetime of the dark matter halo (see Cole et al. 2000). In Font2008a, the yield is a factor of two higher than that adopted in Bower2006a, which gives a better match to observed galaxy colours (Gonzalez et al. 2008). (iii) Baugh2005M adopts a constant density core isothermal profile, in which the core radius evolves with time as low entropy gas cools (see Cole et al. 2000). The cooling radius is defined in the same way as in Bower2006a and Font2008a.

(2) *Gas cooling: AGN heating of the hot halo.* Bower2006a, Font2008a and DeLucia2006a all modify the

² We note, however, that independent algorithms are used to construct the halo merger trees. For a given halo the Durham and Munich merger trees are not necessarily the same.

³ The Millennium galaxy archive can be found at Durham (<http://galaxy-catalogue.dur.ac.uk:8080/Millennium>) or Munich (<http://www.g-vo.org/Millennium>)

cooling flow in massive haloes by appealing to heating from “radio-mode” AGN feedback, following the accretion of material from the cooling flow onto a central supermassive black hole.

(3) *Gas cooling: halo baryon fraction.* In Baugh2005M there is no heating of the hot halo by AGN feedback. Instead, a new channel is introduced for gas heated by the energy released by supernova explosions. Some fraction of the gas, as is common in the majority of semi-analytical models, is reheated and re-incorporated, on some timescale, into the hot gas halo (see Benson et al. 2003). The rest of the reheated gas is ejected from the halo altogether in the superwind. In the Baugh2005 model, this gas is not allowed to re-cool at any stage. This process becomes inefficient in more massive haloes. However, the cooling rate is reduced in such haloes because they have less than the universal fraction of baryons (due to superwind ejection of gas from their progenitors).

(4) *Gas cooling: cooling in satellites.* Font2008a introduced a new cooling scenario based on the hydrodynamical simulations of McCarthy et al. (2008). Traditionally, the ram pressure stripping of the hot gas from a satellite halo has been assumed to be maximally efficient and instantaneous following a merger between two dark matter haloes. McCarthy et al. showed that in gas simulations this is not the case and that the satellite can retain a substantial amount of hot gas, with the fraction depending upon the satellite orbit. McCarthy et al. used a suite of simulations to calibrate a recipe to describe how much hot gas is kept. Font et al. (2008) extended the GALFORM code to include this prescription to calculate the amount of hot gas attached to each satellite galaxy within a halo and to allow the gas to cool directly onto the satellite, rather than onto the central (most massive) galaxy in the main dark matter halo. The other models considered in this paper do not allow gas to cool onto satellite galaxies.

(5) *Galaxy mergers.* Galaxies merge due to dynamical friction. Baugh2005M adopts the form of the merger timescale given by Eq. 4.16 of Cole et al. (2000). Bower2006a and Font2008a use the same prescription with a timescale that is longer by 50%; physically this can be explained as a reduction in the mass of the satellite halo due to tidal stripping. DeLucia2006a use a hybrid scheme in which a satellite galaxy is associated with a substructure halo, which is followed until stripping and disruption result in it dropping below the resolution limit of the simulation. From the last radius at which the substructure was seen, an analytic estimate of the merger time is made, using the dynamical friction timescale (but with a different definition of the Coulomb logarithm) and applying a boost of a factor of 2 (to improve the match to the bright end of the present day optical luminosity function).

(6) *Star formation.* The Durham models allow the star formation timescale to scale according to circular velocity of the disc computed at the half mass radius. The star formation timescale also depends on a timescale parameter which can be held fixed (Baugh2005M) or which can scale with the disc dynamical time (Bower2006a, Font2008a). In the Durham models, all of the cold gas is available for star formation. In DeLucia2006a, a critical mass of cold gas has to be reached before star formation can begin, motivated by the observational inference that star formation requires

a critical surface density of cold gas, as is also motivated theoretically (Kennicutt 1998). Only the cold gas mass in excess of the threshold is available for star formation. The timescale adopted is the disc dynamical time. The models all adopt a standard solar neighbourhood initial mass function (IMF) for quiescent star formation in discs. In the case of Baugh2005M, for episodes of star formation triggered by a galaxy merger a top-heavy IMF is adopted with a correspondingly higher yield and recycled fraction.

(7) *Heating of cooled gas by supernovae.* In the Durham models, the amount of gas reheated by supernova feedback per timestep is a multiple of the star formation rate which depends on the choice of values adopted for the feedback parameters. As we have touched upon in (3) above, in Baugh2005M, the gas reheated by supernovae can either be ejected completely in a superwind, or heated up so that it is later re-incorporated into the hot halo (when a new halo forms i.e. after a doubling of the halo mass). Bower2006a and Font2008a do not consider the superwind channel for reheated gas. These models allow the reheated gas to be added to the hot gas reservoir on a timescale which depends on the halo dynamical time, rather than waiting for a new halo to form. DeLucia2006a follows Croton et al. (2006), who globally pin the rate at which gas is reheated by supernovae to a multiple of the star formation rate suggested by observations. The amount of energy released by supernovae is tracked and used to compute if any of the hot halo is ejected, to be re-incorporated on some timescale.

The models contain parameters which are set by requiring that the predictions reproduce a subset of the available observational data. Different datasets are used in this process and different importance is attached to how well a particular dataset is reproduced e.g. Baugh2005M used the observed gas fractions in spirals to help determine the star formation timescale, whereas as Bower2006a used the colour distribution to set this parameter. The gas fraction in spirals is the only data used to set parameters which explicitly relates to the cold gas content of galaxies (and even then was not used in all the models); other observations, e.g. the galaxy luminosity and mass functions provide indirect constraints on the cold gas content. None of the model parameters have been adjusted for the purposes of this paper, except for the reduction in the baryon density parameter in Baugh2005M, as explained above.

3 BASIC PREDICTIONS

In this Section we present the model predictions for the cold gas mass, radius and rotation speed of galactic discs. These quantities are used in the next section to predict the 21cm luminosity of the galaxies. Here we do not discuss any quantities derived from these direct model outputs, deferring discussion of how we convert from cold gas mass to HI mass to § 4.1.

We begin by inspecting the cold gas mass functions predicted by the four models in Fig. 1 at $z=0$ (upper panel) and $z=1$ (lower panel). For comparison, we show also an observed $z=0$ cold gas mass function (open circles and error bars), obtained by converting the $z=0$ mass function of HI in galaxies from HIPASS (cf. Zwaan et al. 2005) to a cold gas mass function, using the conversion fac-

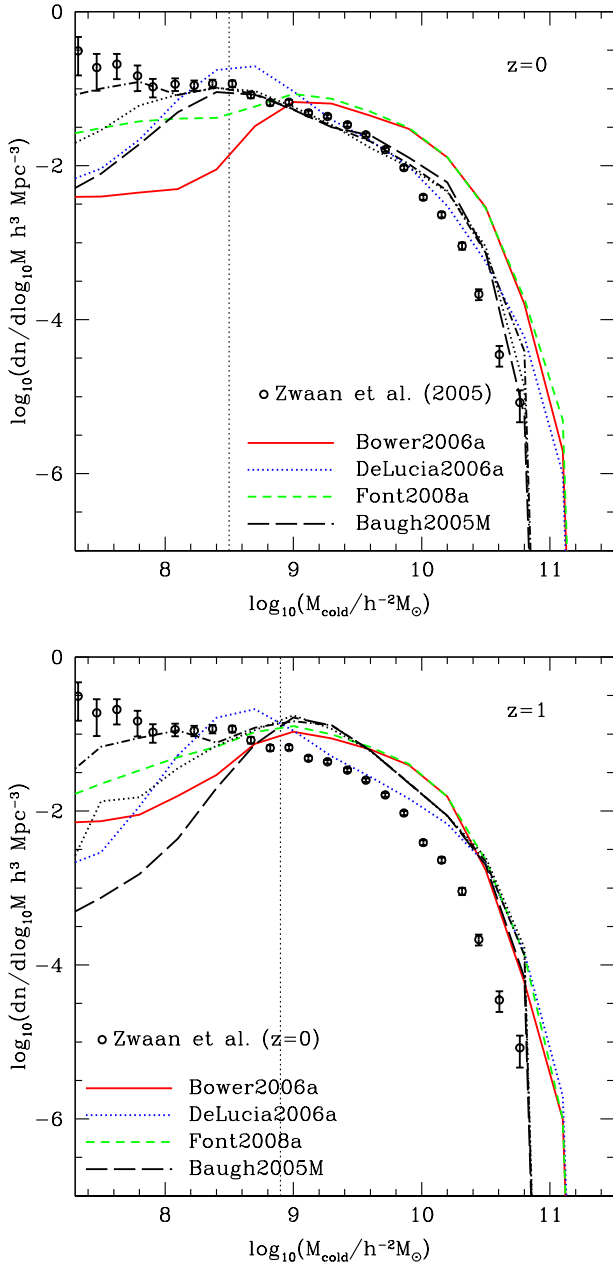


Figure 1. The predicted cold gas mass function at $z = 0$ (top) and $z = 1$ (bottom). The points show an observational estimate of the HI mass function at $z=0$ by Zwaan et al. (2005), converted into a cold gas mass function (see Section 4.1). Different lines correspond to different models as indicated by the legend. For Baugh2005M, the results using the Millennium simulation merger trees are shown by the dashed black line. The dotted and dot-dashed lines show calculations using Monte Carlo merger trees with improved mass resolution (with a mass resolution a factor of 2 and 4 better than the Millennium respectively) but with the galaxy formation parameters held the same. The dotted vertical line indicates the cold gas mass resolution limit of the Millennium galaxy formation models. The cold gas mass resolution limit is slightly higher at $z = 1$ than it is at $z = 0$. In the lower panel, the $z = 0$ data points are repeated for reference.

tor determined in § 4.1. Cold gas masses are plotted in units of $h^{-2} M_{\odot}$ to match the observational units, which depend upon the square of the luminosity distance. We find that DeLucia2006a and Baugh2005M recover the observed $z=0$ mass function reasonably well, following the data closely between $\log_{10}(M_{\text{cold}}/h^{-1} M_{\odot}) \simeq 8.5$ (approximately the cold gas mass resolution limit of the model; see below) and $\log_{10}(M_{\text{cold}}/h^{-1} M_{\odot}) \simeq 9.8$; at larger M_{cold} both models tend to overestimate the amount of cold gas in galaxies by ~ 0.25 dex. In contrast, both Font2008a and Bower2006a predict systematically more cold gas than is observed. This is unsurprising, however, because both Font2008a and Bower2006a also over-predict the gas content in spirals (see for example the discussion in Cole et al. 2000 and their figure 9).

We note that there is a minimum mass below which haloes are not reliably resolved in the Millennium simulation, which imposes a minimum cold gas mass below which the model predictions are unreliable. This arises because the simulation in practice can only resolve dark matter haloes down to some limiting mass and cold gas could be present in haloes less massive than this resolution limit. However, we need to know how the minimum cold gas mass relates to the minimum halo mass; this can be estimated by running Monte Carlo merger trees of different minimum halo masses and comparing with the N-body merger trees. In practice, we run the Baugh2005M model with higher resolution trees generated using the new Monte Carlo prescription of Parkinson et al. (2008) and determine the halo mass down to which the Monte Carlo trees give a good match to the trees extracted from N-body simulations. The cold gas mass functions calculated using the Millennium and Monte Carlo trees diverge below the mass indicated by the dotted vertical line in Fig. 1, at a cold gas mass of $\log(M_{\text{cold}}/h^{-1} M_{\odot}) = 8.5$. In practice, we should repeat this exercise for each model, as the resolution limit may be sensitive to the model recipes. However, given the close agreement between the predictions above this mass limit, we do not expect the variation in the cold gas mass resolution between models to be large.

We note that there is little evolution in the predicted mass functions back to $z = 1$. This is remarkable because it shows that the sources and sinks of cold gas more or less balance one another out. Why might this be so? We expect the sizes of galactic discs to decrease with increasing redshift and so, because star formation proceeds on a dynamical timescale in all of the models except Baugh2005M, it follows that the star formation timescale decreases with increasing redshift. However, gas cools from the hot halo on a timescale that depends on local gas density; because density increases with increasing redshift, it follows that the cooling timescale decreases with increasing redshift. Therefore we expect that the amount of gas to cool per unit time will increase with increasing redshift, but this is offset by the increasing numbers of stars that form per unit time with increasing redshift. Therefore the competing sources (gas cooling) and sinks (star formation and mass ejection by winds) of cold gas balance each other, explaining in a very natural way the lack of evolution in the cold gas mass function.

In Fig. 2 we show how the global density of cold gas ρ_{cold} varies with redshift z . For ease of comparison with observational data, we normalise it by ρ_{crit}/h at $z=0$. Both Bower2006a and Font2008a over-predict the density of cold

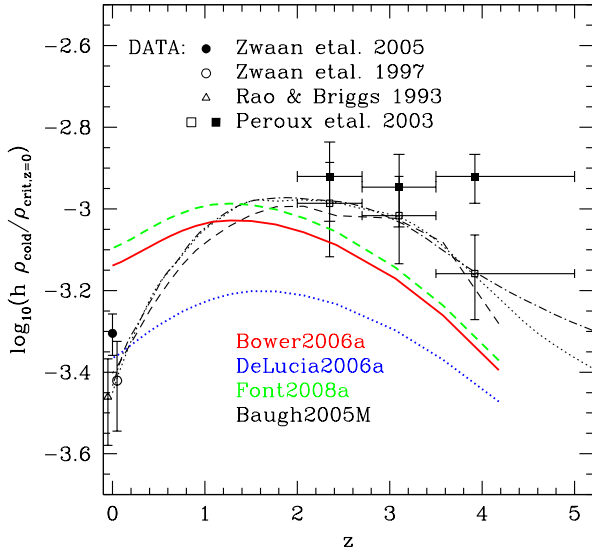


Figure 2. The predicted cold gas density ρ_{cold} , normalised by the $z = 0$ critical density ρ_{crit} , as a function of z . Different lines correspond to different models as indicated by the legend. For Baugh2005M, the results using the Millennium simulation merger trees are shown by the dashed black line. The dotted and dot-dashed lines show calculations using Monte Carlo merger trees with improved mass resolution but with the galaxy formation parameters held the same (see caption of Fig. 1). Filled and open circles correspond to Zwaan et al. (1997); Zwaan et al. (2003) data respectively; open triangles correspond to Rao & Briggs (1993); open and filled squares correspond to Péroux et al. (2003). In the latter case, the open squares indicate the cold gas density inferred from damped Lyman α systems by Péroux et al., and the filled squares show a correction to take into account gas clouds with lower column density.

gas at $z < 1$ and somewhat under-predict the amount of cold gas at higher redshifts. DeLucia2006a predicts a cold gas density that is consistent with observational estimates at $z=0$ but it under-predicts the density at $z > 0$ by a factor of two to three. Of all the models, Baugh2005M most closely matches at all redshifts the observed density of cold gas. Comparing the predictions for this model using the Millennium simulation trees with those from Monte Carlo trees (with improved mass resolution) suggests that the N-body results are robust up to $z \sim 4$.

We now compare the rotation speed of galactic discs as a function of cold gas mass. This is interesting to quantify because it indicates how the velocity width is likely to scale with HI mass, which is important for HI surveys. It also provides a useful insight into how the mean cold gas mass varies as a function of galaxy mass, which can be related to the rotation speed. Fig. 3 shows the rotation speed - disc mass relation at $z = 0$ (top) and $z = 1$ (bottom) predicted by the models. Note that the Durham and Munich models define rotation speed in different ways; in the case of the Durham models, the rotation speed plotted is the circular velocity at the half mass radius of the disc. In the case of the Munich model (DeLucia2006a), the velocity plotted

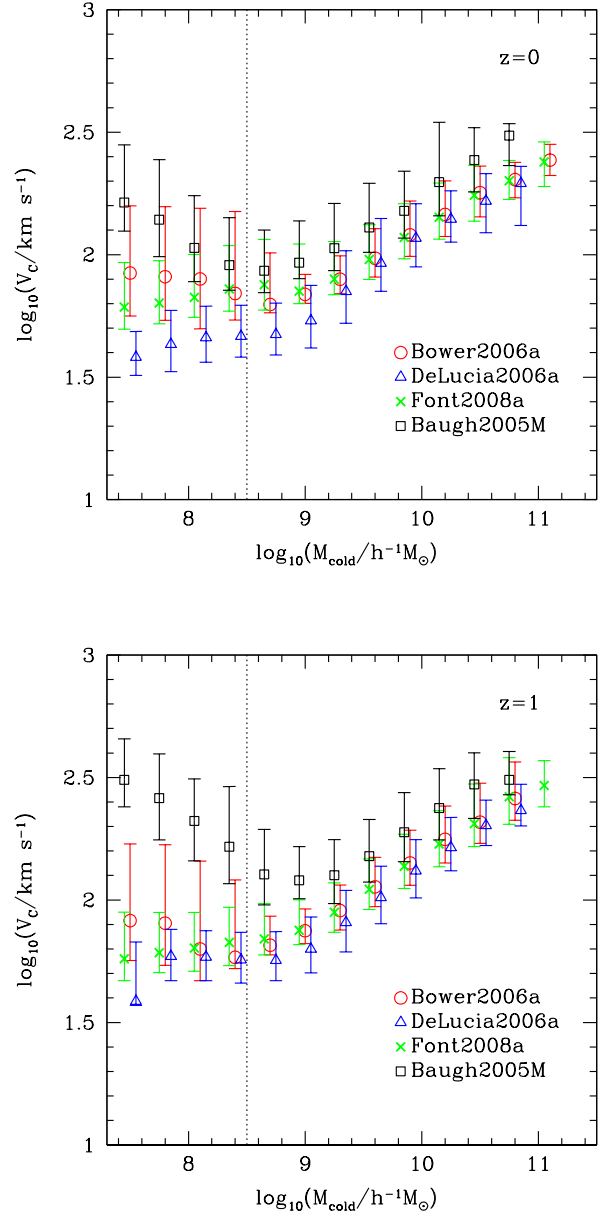


Figure 3. The predicted circular velocity - cold gas mass relation at $z = 0$ (top) and $z = 1$ (bottom). The points shown the median velocity and the bars show the 10-90 percentile range. Different symbols correspond to different models as indicated by the legend. In DeLucia2006, the velocity plotted is measured at the virial radius of the dark matter halo; in the other cases, it is the circular velocity at the half-mass radius of the disc. The dotted vertical line indicates the cold gas mass resolution limit of the Millennium galaxy formation models.

is measured at the virial radius of the dark matter halo. The relation between these two velocities depends upon the mass and distribution of the cold gas and stars in the disc and bulge and of the dark matter. In Bower2006, we find that for L_* galaxies, the circular velocity at the half mass radius is typically 20% higher than that measured at the virial radius for L_* galaxies. After allowing for this differ-

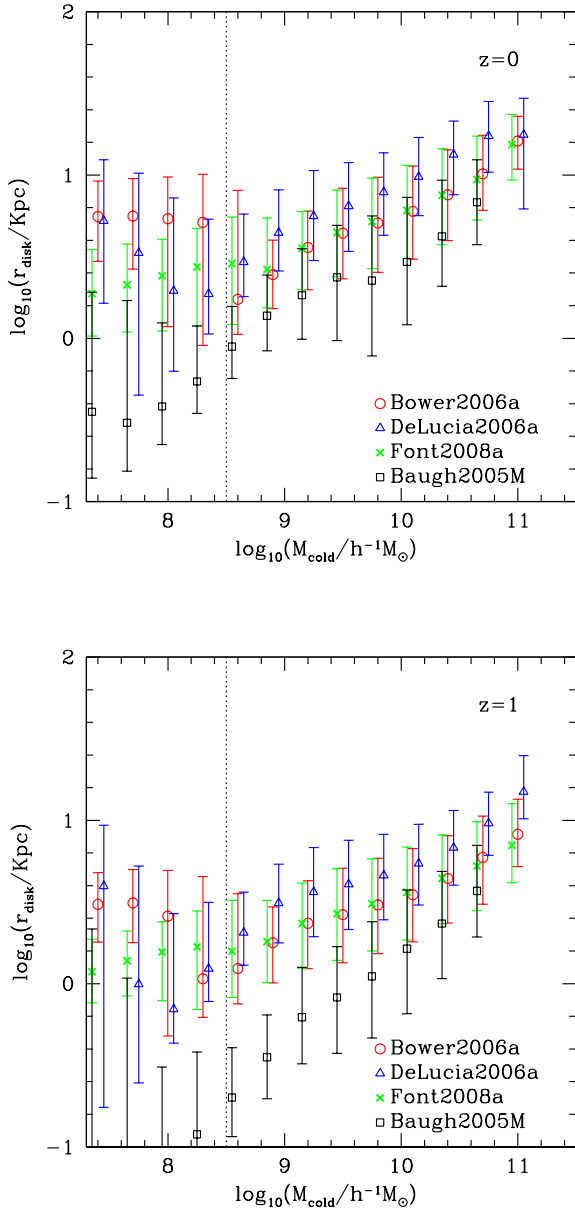


Figure 4. The predicted radius - cold gas mass relation at $z = 0$ (top) and $z = 1$ (bottom). The points show the median velocity and the bars show the 10-90 percentile range. Different symbols correspond to different models as indicated by the legend. The radius plotted is the half mass radius of the disc. In DeLucia2006, the quantity stored in the Millennium Archive is three times the scale length of the exponential disc, which we convert to a half-mass radius. The dotted vertical line indicates the cold gas mass resolution limit of the Millennium galaxy formation models.

ence, the DeLucia2006a rotation speed-cold gas mass relation is in close agreement with the predictions of Bower2006a and Font2008a. This level of agreement is quite remarkable given the differences in the implementations of the physical ingredients in the models. Baugh2005M predicts a rotation speed that is higher than the other models by around 50%. One possible explanation is that the discs are more concen-

trated in this model, which is indeed the case in Fig. 4 (see below). The model predictions diverge from each other below a cold gas mass of $\log(M_{\text{cold}}/h^{-1}M_{\odot}) = 8.5$ and there is a change in the slope of the rotation speed - cold gas mass relation below this mass. This is the minimum mass down to which the predictions from the Millennium simulation merger trees are reliable. There is very little evolution in the circular velocity - cold gas mass relation between $z = 0$ and $z = 1$; the zero-point of the $z = 1$ relation is about 25% higher.

The predicted relation between disc radius and the cold gas mass of the disc is plotted in Fig. 4. The radius plotted for the Durham models is the half mass radius of the disc. This takes into account conservation of the angular momentum of the cooling gas and the dynamical equilibrium of the disc, bulge and dark matter; see Almeida et al. (2007) and Gonzalez et al. (2008) for details for this calculation. For DeLucia2006a, the quantity stored in the Millennium Archive is three times the scale length of the exponential disc, which is computed by scaling from the virial radius of the dark matter halo (for a comparison of the size of disc dominated galaxies in Baugh2005M and Bower2006a, see Gonzalez et al. 2008). We have converted this length to a half mass radius to plot on Fig. 4. The DeLucia2006a half-mass radii computed in this way are approximately 0.2 – 0.3dex larger than those predicted by Bower2006a and Font2008a. Given the differences in the way the disc sizes are computed in the models it is perhaps surprising that the DeLucia2006a, Bower2006a and Font2008a predictions are so close. One might expect the Durham predictions to be smaller than those from the Munich model, because the former take into account the gravitational contraction of the dark matter and the self-gravity of the disc and bulge. Baugh2005M predicts smaller gas discs than the other models. However, this model also predicts sizes for stellar discs that are in much better agreement with observational data at $z = 0$ than the other models (Gonzalez et al. 2008). As with the rotation speed - cold gas mass relation, there is little evolution in the radius - cold gas mass relation between $z = 0$ and $z = 1$. The model predictions diverge from one another below the mass resolution of $\log(M_{\text{cold}}/h^{-1}M_{\odot}) = 8.5$.

4 IMPLICATIONS FOR HI SURVEYS

The results presented so far encapsulate what current semi-analytic galaxy formation models can tell us about the distribution of cold gas masses of galaxies as a function of redshift. We can use this information to deduce the distribution of HI masses of galaxies, from which we can predict number counts of HI sources as a function of redshift. These predictions can then be compared with forthcoming HI surveys on the SKA path-finders, such as ASKAP, MeerKAT and APERTIF, and ultimately on the SKA.

Such a comparison represents an important and fundamental test of the semi-analytic galaxy formation framework. Semi-analytic model parameters are calibrated explicitly to reproduce statistical properties of the observed galaxy population where observational data exist such as the galaxy luminosity function (e.g. Benson et al. 2003) and the abundance of sub-mm galaxies at high redshift (e.g. Baugh et al. 2005). However, this approach is sometimes criticised pre-

cisely because it is calibrated to reproduce properties of the observed galaxy population. It is not always clear how robust model predictions are if the parameters have been adjusted to match as many observational datasets as possible. Few observed data exist for the HI properties of galaxies at redshifts $z \gtrsim 0.05$ and so such data will provide a compelling test of the currently favoured models we consider in this paper.

In this section we use the cold mass functions presented in the previous section to predict HI source number counts for forthcoming HI surveys. To do this, we must first convert cold gas masses, which are the natural outputs of the models, to HI masses. Then we consider how the sensitivity and angular resolution of a radio telescope affects whether or not a particular galaxy at a given redshift is likely to be detected in a given HI survey. Finally we investigate the impact of sensitivity on the number counts of HI galaxies and we assess the angular resolution required to resolve gas-rich galaxies out to $z \sim 3$.

4.1 Conversion of Cold Gas Mass to HI Mass

We adopt a simple and clean approach to converting cold gas mass to HI mass, which follows that of Baugh et al. (2004). Firstly, we note that $\sim 24\%$ by gas mass is helium; and secondly, a fraction of the neutral hydrogen will be molecular (H_2) rather than atomic (HI). We ignore the fraction of ionised gas in galaxy discs because this is very small. We assume that this molecular fraction is the same for all galaxies, which means that a simple uniform scaling can be applied to the cold gas mass functions presented in the previous section to obtain HI mass functions. This is a simplification because we expect that this fraction will vary somewhat between galaxies and will be influenced by environment and morphological type (see, for example, the recent detailed analyses of Obreschkow & Rawlings 2009 and Obreschkow et al. 2009b). However, we feel that our simple approach is justified on the basis that it is transparent (i.e. we do not need to introduce yet more parameters) and it allows for easier comparison between the different models.

Keres et al. (2003) measured the luminosity of CO, a widely used tracer of H_2 from which its physical density can be deduced (see, for example, Spitzer 1978; Young & Scoville 1991). They find a cosmological mean H_2 density $\rho_{H_2} = (3.1 \pm 0.9) \times 10^7 h M_\odot \text{Mpc}^{-3}$. Combining this with the mass density of HI from HIPASS, $\rho_{HI} = (8.1 \pm 1.3) \times 10^7 h M_\odot \text{Mpc}^{-3}$ (cf. Zwaan et al. 2005), we estimate that the ratio of molecular to atomic hydrogen is $\simeq 0.4$, and so we adopt a conversion factor of $M_{HI} = 0.76 M_{\text{cold}}/(1+0.4) \simeq 0.54 M_{\text{cold}}$.

4.2 Detection of HI Sources

Two issues are key in determining whether or not an HI source will be detected reliably by a radio telescope or interferometer; namely, sensitivity and angular resolution. An HI source has an intrinsic luminosity that depends primarily on its HI mass M_{HI} which, along with its line-of-sight velocity width ΔV_{los} and distance D , determines the flux at the position of the observer. The observer measures this flux with a receiver that has finite sensitivity determined

primarily by its effective collecting area A_{eff} and the system temperature T_{sys} , and it is this limiting sensitivity that determines whether or not the source is detected. Note, however, that angular resolution also plays an important role; HI 21-cm emission from a galaxy is likely to be spatially extended and an extended source can be “resolved out” by an interferometer if it is observed with too high an angular resolution. In the next two sections we consider how sensitivity and angular resolution affect HI source number counts.

4.2.1 Sensitivity

If we could construct the ideal radio telescope with arbitrarily high sensitivity, then we would observe a flux S_{obs} from an HI source at redshift z . This is determined by the source’s HI mass M_{HI} , its velocity width ΔV_{los} and redshift z . The relationship between S_{obs} and M_{HI} , ΔV_{los} and z can be obtained as follows.

The emissivity ϵ_{ν_0} at rest-frame frequency ν_0 tells us the rate at which energy is emitted by an HI source at this frequency per unit volume per steradian. We can express this as

$$\epsilon_{\nu_0} = \frac{1}{4\pi} h\nu_0 A_{12} \frac{n_2}{n_H} n_H \phi(\nu_0), \quad (1)$$

where $h\nu_0$ is the energy of the 21-cm photon (h is Planck’s constant and ν_0 is the photon frequency), n_2/n_H tells us what fraction of atoms are expected to be in the upper state, A_{12} is the Einstein coefficient which tells us the spontaneous rate of the transition from the upper to lower state, n_H is the total number density of hydrogen atoms in the source and $\phi(\nu)$ is the line profile. We expect $n_2/n_H \simeq 3/4$ because the temperature of the cloud corresponds to a much larger energy than the energy difference corresponding to the transition from the upper to lower state (ie. $kT \gg h\nu$, cf. Spitzer 1978). Integrating over a solid angle of 4π steradians and over the volume of the source gives us the luminosity at frequency ν_0 , L_{ν_0} ,

$$L_{\nu_0} = \frac{3}{4} h\nu_0 A_{12} \frac{M_{HI}}{m_H} \phi(\nu_0), \quad (2)$$

where we write the number of hydrogen atoms as M_{HI}/m_H , m_H being the mass of the hydrogen atom.

When we observe 21-cm emission from an HI source, the radiation arises from a forbidden transition, which implies a small natural line width (5×10^{16} Hz). Therefore the observed line profile $\phi(\nu_0)$ is in practice determined by Doppler broadening due to the motions of HI atoms in the galaxy, which, in disc galaxies, are dominated by the large-scale rotational velocity. We therefore assume that $\phi(\nu_0)$ can be approximated as a top hat function of width $\Delta\nu_0 = (\Delta V_{\text{los}}/c)\nu_0$ and height $1/\Delta\nu_0$. Noting this, we can write the total monochromatic flux at the position of the observer as

$$S_\nu = (1+z) \frac{L_{\nu(1+z)}}{4\pi D_L(z)^2}; \quad (3)$$

here $\nu = \nu_0(1+z)^{-1}$ is the redshifted frequency measured by the observer and $D_L(z) = (1+z) D_{\text{co}}(z)$ is the luminosity distance of the source with respect to the observer ($D_{\text{co}}(z)$ is the radial comoving separation between source and observer). Therefore the measured flux at the position of the observer is

$$S_{\text{obs}} \Delta\nu = \frac{3}{16\pi} \frac{h\nu A_{12}}{m_{\text{H}}} M_{\text{HI}} \frac{1}{D_L(z)^2} (1+z), \quad (4)$$

which we rewrite as

$$S_{\text{obs}} = \frac{3}{16\pi} \frac{hcA_{12}}{m_{\text{H}}} M_{\text{HI}} \frac{1}{D_L(z)^2} \frac{1}{\Delta V_{\text{los}}} (1+z). \quad (5)$$

Here we assume that $\Delta\nu$ in equation 4 can be written as

$$\Delta\nu = \frac{\Delta\nu_0}{1+z} = \frac{\Delta V_{\text{los}}}{c} \frac{\nu_0}{1+z}, \quad (6)$$

where ΔV_{los} is the rest-frame line-of-sight velocity width of the galaxy. ΔV_{los} will depend on the inclination i of the disc, varying as $2V_c \sin i$ where V_c is the disc circular velocity, and $i = 0$ or $\pi/2$ correspond to a face-on or edge-on disc respectively. In our analysis we assume that galaxy discs have random inclinations with respect to the observer, with an average velocity width of $\sim 1.57 V_c$ (cf. § 4.3).

The measured flux from the source must be compared with the intrinsic limiting sensitivity of the receiver. Assuming a dual polarisation radio receiver, the limiting root mean square flux S_{rms} can be calculated in a straightforward manner (cf. Burke & Graham-Smith 1996);

$$S_{\text{rms}} = \frac{2k_B T_{\text{sys}}}{A_{\text{eff}} \sqrt{2\Delta\nu_{\text{rec}}\tau}}, \quad (7)$$

where A_{eff} is the total (effective) collecting area of the telescope, T_{sys} is the system temperature, $\Delta\nu_{\text{rec}}$ is the bandwidth used in the receiver, τ is the integration time and k_B is Boltzmann's constant. The effective area A_{eff} and system temperature T_{sys} are the key parameters. The SKA will have an effective area⁴ of order $A_{\text{eff}}=1 \text{ km}^2$ and its pathfinders will have effective areas of $f_{\text{SKA}} \text{ km}^2$; for pathfinders such as ASKAP, MeerKAT and APERTIF, $f_{\text{SKA}} \lesssim 0.01$. A conservative estimate of the system temperature would be $T_{\text{sys}} = 50\text{K}$. We can rewrite Eq. (7) as

$$\frac{S_{\text{rms}}}{1.626\mu\text{Jy}} = \left(\frac{A_{\text{eff}}}{\text{km}^2}\right)^{-1} \left(\frac{T_{\text{sys}}}{50\text{K}}\right) \left(\frac{\Delta\nu_{\text{rec}}}{\text{MHz}}\right)^{-1/2} \left(\frac{\tau}{\text{hr}}\right)^{-1/2}, \quad (8)$$

where $1\text{Jy} = 10^{-26} \text{ W m}^{-2} \text{ Hz}^{-1}$. The limiting flux sensitivity of the telescope S_{lim} is then $S_{\text{lim}} = n_\sigma S_{\text{rms}}$, where n_σ defines the threshold for a galaxy to be reliably detected. Once we have fixed the integration time τ and the bandwidth $\Delta\nu_{\text{rec}}$, we have the limiting sensitivity of our radio telescope.

It is worth reminding us of the relationship between the frequency bandwidth $\Delta\nu_{\text{rec}}$ in equations 7 and 8, which is particular to the radio telescope, and the frequency width $\Delta\nu$ in equations 4 and 5, which is set by the velocity width of the HI line ΔV_{los} . If we are to maximise the signal-to-noise ratio for detecting the galaxy in a survey, then it is important that these bandwidths are matched. The overall telescope frequency bandwidth at a given frequency will be broad – typically $\gtrsim 100 \text{ MHz}$ – and much greater than the velocity width of an individual galaxy (e.g. $\sim 1 \text{ MHz}$ corresponds to a $\sim 200 \text{ km s}^{-1}$ galaxy), but the overall bandwidth consists of $\sim 10^3$ to 10^4 frequency channels that are much narrower than the expected frequency width of a galaxy.

⁴ Despite its name, it is unlikely that the SKA will have an area of 1 km^2 ; instead it is likely to be $\sim 0.5 \text{ km}^2$, which ensures greater survey speed at the expense of sensitivity.

Therefore a single telescope pointing will produce a huge data cube centred on a frequency ν with an overall bandwidth that consists of thousands of narrower frequency channels $\delta\nu$. These channels will then be re-binned to produce data cubes with different frequency resolutions $\Delta\nu_{\text{rec}}$, and one of these re-binnings will have $\Delta\nu_{\text{rec}} \simeq \Delta\nu$, which will be optimal for detecting an individual galaxy of a given velocity width with a sufficiently high signal-to-noise.

4.2.2 Angular Resolution

The angular resolution of the radio telescope becomes important when the HI source is extended rather than a point source. For a single dish telescope the angular resolution is $\sim \lambda/D$, where λ is the wavelength of the radiation and D is the diameter of the dish. Sources with angular sizes θ smaller than this are indistinguishable from point sources. For radio interferometers it is the lengths of the baselines between pairs of dishes B rather than the diameters of individual dishes that dictate the angular resolution. If the longest baseline is B_{max} and the shortest is B_{min} , then the interferometer will resolve angular scales roughly from $\Theta_{\text{min}} = \lambda/B_{\text{max}}$ to $\Theta_{\text{max}} = \lambda/B_{\text{min}}$. Interferometers can therefore provide higher angular resolution than a single dish, which is desirable because it allows for HI sources to be mapped in greater detail. However, sources more extended than $\sim \Theta_{\text{max}}$ get “resolved out”, and have their fluxes underestimated. The fraction of a galaxy's flux that is resolved out will depend on, for example, the precise distribution of interferometer baselines and what one assumes for the surface brightness profile of the galaxy (see, for example, the discussion in Abdalla et al. 2009). In the case of the SKA, the shortest baseline is expected to be 20m, which corresponds to an angular resolution of $\Theta_{\text{max}} \sim 2100''$ at $\lambda=21 \text{ cm}$, while maximum baseline will be $\gtrsim 3000 \text{ km}$, which corresponds to a resolution $\Theta_{\text{min}} \sim 0.1''$. As we will see in §4.3, the predicted HI sizes of galaxies in cosmological surveys are typically of order arcsecs or smaller, so there should not be any problem in practice with galaxies being “resolved out”.

4.3 Predictions for Observables

First, we examine the predictions of the four models for the number counts dN/dz of HI galaxies per square degree of sky as a function of redshift. By number counts, we mean the number of HI sources dN that can be detected in a redshift interval dz centred on a redshift z ,

$$\frac{dN}{dz} = \frac{dV}{dz} \int_0^\infty \frac{dn}{dM} f(M) dM. \quad (9)$$

where dV/dz is the cosmological volume element at redshift z , dn/dM is the HI mass function at z and $f(M)$ represents the fraction of galaxies with HI mass M that can be detected by the radio telescope. For simplicity we assume that $f(M)$ depends only on limiting sensitivity, which depends on M_{HI} . The angular resolution of the telescope also plays a role but its influence on $f(M)$ requires further assumptions to be made about, for example, the distribution of baselines, the clumpiness of HI within galaxy, its surface density profile, etc... and so we ignore this dependence.

In estimating predicted number counts, we assume a survey lasting $\tau=1$ year on a radio telescope with an effec-

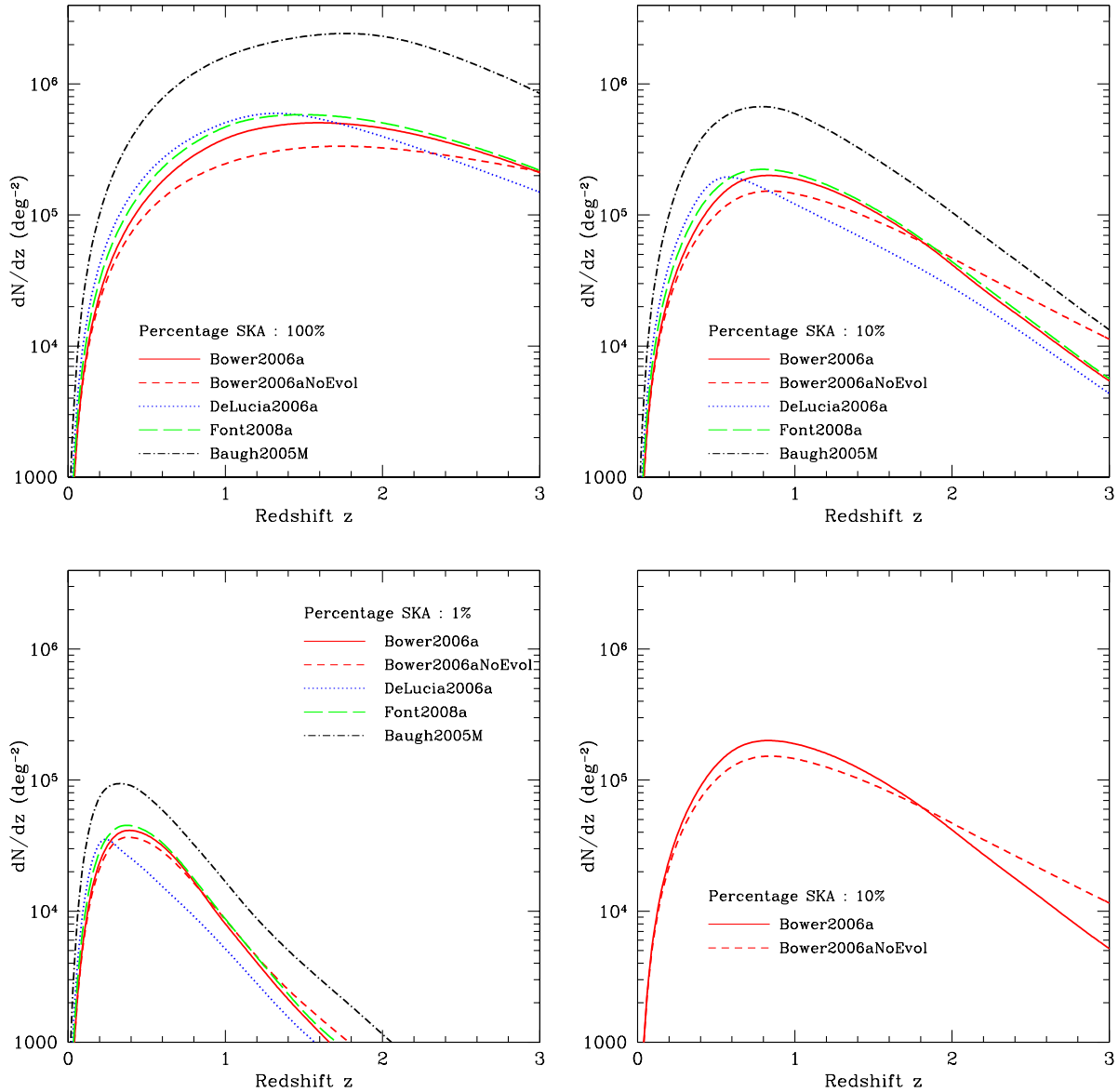


Figure 5. Number counts of galaxies per square degree per unit redshift for a telescope with 100% (top left), 10% (top right) and 1% (bottom left) of the effective area of a fiducial SKA ($A_{\text{SKA}} = 1 \text{ km}^2$), for a deep HI survey lasting 1 year. Only sources that satisfy $S_{\text{obs}} \geq n_{\sigma} S_{\text{rms}}$ with $n_{\sigma} = 10$ are included. Note that we do not include galaxies with cold gas masses below the resolution limit of $\log(M_{\text{cold}}/h^{-1} M_{\odot}) = 8.5$. The bottom right panel highlights how the counts change in Bower2006a if we assume a “No Evolution” case in which the $z = 0$ mass function applies at all redshifts, for a 10% SKA. For reference we show also “No Evolution” curves for Bower2006 in the other cases.

tive area $A_{\text{eff}} = f_{\text{SKA}} \text{ km}^2$, where $f_{\text{SKA}} = 1$ for the fiducial SKA. We focus on $f_{\text{SKA}} = 0.01, 0.1$ and 1 , corresponding to a 1%, 10% and 100% SKA⁵. The measured flux S_{obs} from a galaxy is estimated using equation 5. The velocity width ΔV_{los} is taken to be $2V_{\text{c,half}} \sin i$, where $V_{\text{c,half}}$ is the circular velocity at the half-mass radius of the galaxy. Galaxies are given random inclinations i , drawn from a uniform distribution in $\cos i$. The measured flux is compared to the limiting flux S_{rms} (equation 7) on a galaxy-by-galaxy basis

(assuming $\Delta \nu_{\text{rec}} = \Delta \nu$ and using equation 6 to estimate $\Delta \nu$) to estimate the signal-to-noise ratio. Our criterion for detection is $S_{\text{obs}}/S_{\text{rms}} \geq n_{\sigma} = 10$.

Fig. 5 shows how the number counts of HI galaxies varies with redshift for surveys with A_{eff} of 100% A_{SKA} (top left hand panel), 10% A_{SKA} (top right hand panel) and 1% A_{SKA} (bottom left hand panel). A_{eff} is crucial in determining how many galaxies can be detected and the range of redshifts that can be probed. We find the number counts peak at $\sim 4 \times 10^4 / 2 \times 10^5 / 5 \times 10^5$ galaxies per square degree at

⁵ Although, as noted previously, the final SKA is likely to have an effective area smaller than 1 km^2 .

$z \sim 0.4/0.8/1.4$ for a year long HI survey on a 1%/10%/100% SKA.

A couple of interesting trends are immediately apparent in this figure. The first is that DeLucia2006a, Bower2006a and Font2008a, which all incorporate a form of AGN feedback, all predict broadly similar number counts out to $z \sim 3$. There are differences in the details that reflect differences between the models that can be readily inferred from the mass functions shown in Fig. 1. For example, DeLucia2006a predicts enhanced number counts at lower redshifts and depressed number counts at intermediate to high redshifts with respect to Bower2006a and Font2008a. Here lower, intermediate and higher are defined relative to the redshift at which the number counts peak – approximately $z \sim 0.5, 1.0$ and 1.5 for 1%, 10% and 100% A_{SKA} respectively. The second is that Baugh2005M, consistently predicts many more gas-rich galaxies than the other three models. There are several reasons for this: (1) Baugh2005M incorporates galactic super-winds rather than AGN feedback, which affects the cooling rate in massive haloes; (2) Baugh2005M uses weaker supernovae feedback than the other models; and (3) the star formation timescale in galactic discs does not scale with the disc dynamical time in Baugh2005M, whereas it does in the other models.

The bottom right hand panel of Fig. 5 makes clear the impact on the number counts of approximating the HI mass function at $z > 0$ by the $z=0$ HI mass function. We focus on Bower2006a for a 10% A_{SKA} 1 year all-sky survey. The solid curve shows the number counts in the standard Bower2006a, in which the HI mass function evolves over time, whereas the dashed curve shows the number counts which result in the Bower2006aNoEvol approximation, in which the HI mass function at a given z is replaced by the HI mass function measured at $z=0$. Over the redshift range $0 \lesssim z \lesssim 2$ this would appear to be a reasonable approximation to make – the discrepancy is greatest at $z \sim 1$ where the Bower2006aNoEvol approximation underestimates the number counts by a factor of ~ 2 . At $z \gtrsim 2$ the Bower2006aNoEvol approximation diverges from Bower2006a and by $z \sim 3$ the discrepancy is a factor of ~ 10 . For reference, we plot also the “No Evolution” prediction for Bower2006a (dashed curves) in the 1%, 10% and 100% A_{SKA} panels.

Fig. 6 and Fig. 7 show how the angular size of HI galaxies varies with redshift. We compute the angular diameter as $\theta = 2 R_h / D_{\text{ang}}$ where R_h is the half mass radius of the galaxy and $D_{\text{ang}}(z) = (1+z)^{-1} D_{\text{co}}(z)$ is the angular diameter distance of the galaxy with respect to the observer, where, as before, $D_{\text{co}}(z)$ is the radial comoving separation between source and observer. The points correspond to the median angular diameters while the upper and lower errorbars indicate the 25th and 75th percentiles of the angular diameter distributions at that redshift. Points are given horizontal offsets of 0.025 in redshift to aid clarity. In Fig. 6 we plot the redshift dependence of the median angular diameters of galaxies with HI masses $M_{\text{HI}} \geq 10^9 h^{-1} M_\odot$ (upper panel) and $M_{\text{HI}} \geq 10^{10} h^{-1} M_\odot$ (lower panel) varies with redshift out to $z \lesssim 3$. In Fig. 7 we focus on the variation predicted by Baugh2005 and DeLucia2006a for galaxies with $M_{\text{HI}} \geq 10^9 h^{-1} M_\odot$ over the redshift interval $0 \leq z \leq 1$.

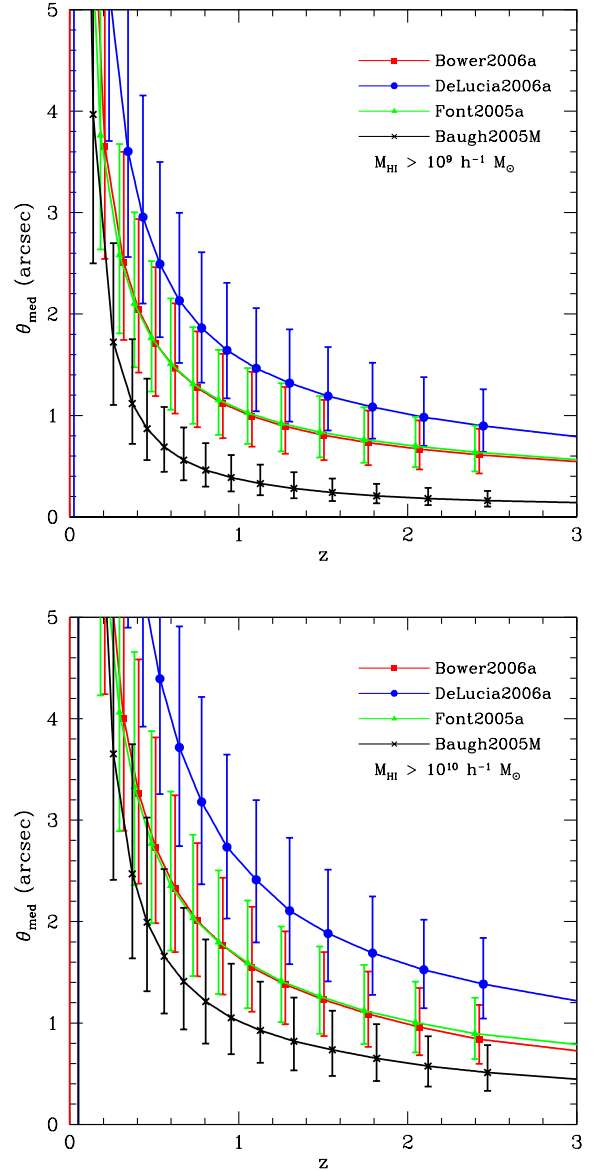


Figure 6. The predicted redshift variation of the angular diameter of galaxies with HI masses $M_{\text{HI}} \gtrsim 10^9 h^{-1} M_\odot$ (upper panel) and $M_{\text{HI}} \gtrsim 10^{10} h^{-1} M_\odot$ (lower panel). Different symbols correspond to different models, as indicated by the legend.

Knowledge of the expected redshift variation of angular diameter of an extended HI source is useful because it allows one to estimate the number of sources that are likely to be resolved out. Fig. 6 and Fig. 7 distill the information presented in Fig. 4, where we showed how the half mass radii of galaxies varied with cold gas mass at a given redshift. The models indicate that galaxies that have larger HI masses tend to have larger half mass radii, which corresponds to more extended angular diameters at a given redshift. The angular diameter decreases sharply between $z=0$ and $z \simeq 0.5$, and more gently at $z \gtrsim 0.5$. The median angular size varies between $5''$ and $10''$ at $z=0.1$, $1''$ and $3''$ at $z=1$ and $1''$ and $3''$ at $z=3$ for galaxies with HI masses in excess of $10^9 h^{-1} M_\odot$; the upper and lower bounds correspond to the predictions

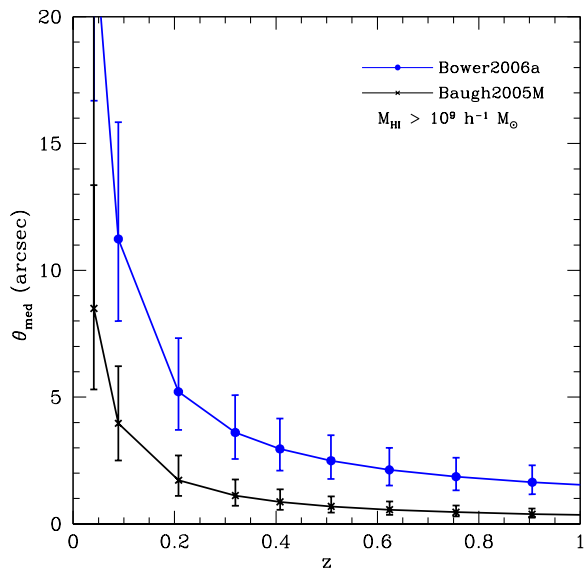


Figure 7. The predicted redshift variation of the angular diameter of galaxies with HI masses $M_{\text{HI}} \gtrsim 10^9 h^{-1} M_{\odot}$ at $z \lesssim 1$ in Baugh2005M and DeLucia2006a.

from DeLucia2006a and Baugh2005M. Therefore, to resolve a typical galaxy with an HI mass of $M_{\text{HI}} \gtrsim 10^9 h^{-1} M_{\odot}$ at $z \sim 1$ requires a maximum baseline of order 100 km.

5 SUMMARY

Neutral atomic hydrogen is the fundamental baryonic building block of galaxies and understanding how its abundance varies over cosmic time will provide us with important insights into galaxy formation. Few observational data exist for the abundance of neutral hydrogen at redshifts beyond $z \gtrsim 0.05$, the extent of the HIPASS survey (Meyer et al. 2004), but this will change with the advent of the Square Kilometre Array, which will see first light by about 2020. The SKA will transform cosmology and galaxy formation (e.g. Blake et al. 2004; Braun 2007), allowing us to probe the cosmic HI distribution out to redshifts $z \sim 3$. In the meantime, HI surveys on SKA path-finders such as ASKAP (Johnston et al. 2008), MeerKAT (Jonas 2007) and APER-TIF (Verheijen et al. 2008) will provide us with important initial glimpses into the cosmic HI distribution out to redshifts $z \sim 1$. Because we have such few observational data for the cosmic HI distribution beyond $z \sim 0.05$, the coming decade promises to provide powerful tests of the predictions of theoretical galaxy formation models. It is therefore timely to ask what galaxy formation models predict for the abundance of neutral hydrogen in galaxies.

In this paper we have investigated four of the currently favoured galaxy formation models – those of Baugh et al. (2005), Bower et al. (2006), De Lucia & Blaizot (2007) and Font et al. (2008) – and determined what they predict for the mass function of cold gas in galaxies and how it evolves with redshift. Each of the models use merger trees derived from the Millennium Simulation (cf. Springel et al. 2005) and so any differences between the model predictions re-

fect intrinsic differences in the models themselves. Three of the models (Baugh2005M, Bower2006a and Font2008a) use the Durham semi-analytic code GALFORM (cf. Cole et al. 2000) whereas the fourth (DeLucia2006a) uses the Munich semi-analytic code. Arguably the most important difference between the models is in the precise treatment of feedback; Bower2006a, DeLucia2006a and Font2008a all incorporate a form of AGN feedback whereas Baugh2005M does not, instead favouring galactic super-winds.

Interestingly we find that the model predictions are broadly consistent with one another. Differences between the models reflect (1) the use of AGN heating to suppress gas cooling in massive haloes (which is used in Bower2006a, Font2008a and DeLucia2006a but not in Baugh2005M, which invokes supernovae driven super-winds); (2) the strength of supernovae feedback, which is weakest in Baugh2005M; and (3) the scaling (or not) of the star formation timescale in galactic discs with the disc dynamical time, which is not adopted in Baugh2005M.

We have focused on three particular aspects of the cold gas properties of galaxies, namely the mass function of cold gas in galaxies and the relationship between a galaxy’s cold gas mass and its half-mass radius and the circular velocity at this radius.

Mass function of cold gas in galaxies: The predictions of Font2008a and Bower2006a are generally very similar, with differences only apparent at small cold gas masses. This is unsurprising because Font2008a descends directly from Bower2006a, the principal difference between the models being the improved treatment of gas stripping by the hot intra-cluster medium in more massive galaxies in Font2008a. At $z=0$ we find that Bower2006 and Font2008 systematically over-predict the numbers of galaxies with HI masses in excess of $10^9 h^{-2} M_{\odot}$ when compared to the observed mass function derived from HIPASS (cf. Zwaan et al. 2005), while Baugh2005M and DeLucia2006a do a reasonably good job of describing the observations. Interestingly we find that the cold gas mass function shows little evolution out to redshifts of $z \simeq 3$ in all four models.

Relationship between cold gas mass and half-mass radius, circular velocity: We have looked at how the half mass radius of galaxies varies with cold gas mass. As we might expect, both Font2008a and Bower2006a predict half mass radii that are in excellent agreement with each other. What is reassuring, however, is the good agreement between Font2008a, Bower2006a and DeLucia2006a. DeLucia2006a derives from the Munich framework and as described in § 2 there are a number of subtle (and some not so subtle) differences between the respective underlying frameworks; for example, the spatial distribution of gas within haloes. Baugh2005M predicts that galaxies have half mass radii that are systematically smaller at a given HI mass than their counterparts in Bower2006a, DeLucia2006a and Font2008a. These trends are reflected in the relations between disc circular velocity (measured at the half mass radius) and cold gas mass – discs in Baugh2005M have systematically higher circular velocities.

We have taken the predicted mass functions of cold gas in galaxies and used them to derive number counts of HI

galaxies for future all-sky HI surveys. Rather than adopting a specific design, we considered surveys carried out on radio telescopes with effective collecting areas A_{eff} that are fractions of the Square Kilometre Array $A_{\text{SKA}} = 1\text{km}^2$; we focused on A_{eff} 1%, 10% and 100% A_{SKA} and assumed that the survey lasted for 1 year. The effective area plays a crucial role in determining the sensitivity S_{rms} of a radio telescope, which in turn is pivotal in determining how many HI galaxies are detected. SKA path-finders such as ASKAP, MeerKAT and APERTIF will have effective areas of order $\sim 1\%$.

The cold gas mass functions were converted to HI mass functions using the simple scaling adopted in Baugh et al. (2004), by multiplying the gas mass by a constant factor of 0.54. We computed the observed flux S_{obs} for each galaxy using both its HI mass and its circular velocity at the half-mass radius to define its velocity width and required that $S_{\text{obs}} \geq 10S_{\text{rms}}$ for the galaxy to be detected. As for the cold gas mass functions, we find that the models that include a form of AGN feedback predict broadly similar number counts; Baugh2005M predicts many more gas rich galaxies, as many as a factor of $\sim 2-3$ more at the redshift at which the number counts peak. Interestingly we find that approximating the HI mass function at $z \lesssim 2$ by the $z=0$ HI mass function has little impact on the number counts one might expect to measure.

In addition, we estimated the dependence of the median angular diameter of HI galaxies on redshift, for galaxies with HI masses $M_{\text{HI}} \geq 10^9 h^{-1} M_{\odot}$ and $M_{\text{HI}} \geq 10^{10} h^{-1} M_{\odot}$. This is useful to know because it allows one to estimate the fraction of the flux that is likely to be lost because it has been resolved out. The models indicate that galaxies with larger HI masses tend to have larger half mass radii and therefore more extended angular diameters at a given redshift. We found that the angular diameter decreases sharply between $0 \lesssim z \lesssim 0.5$ and more gently at $z \gtrsim 0.5$. The median angular size varies between $5''$ and $10''$ at $z=0.1$, $0.5''$ and $3''$ at $z=1$ and $0.2''$ and $1''$ at $z=3$ for galaxies with HI masses in excess of $10^9 h^{-1} M_{\odot}$, where the lower and upper limits correspond to the predictions of Baugh2005M and DeLucia2006a.

We have concentrated on the most straightforward measurement one can make in future HI surveys, namely the number counts of galaxies. However, we expect that the spatial distribution of HI should be a strong function of local galaxy density. For example, we might expect that a galaxy will lose its HI as a result of ram pressure stripping in dense intra-cluster media; this would become apparent as a quenching of the star formation (e.g. Balogh et al. 2000; Quilis et al. 2000), but it should also be evident in an environmental dependence of a galaxy's HI properties.

There is interesting albeit tentative observational evidence to suggest that the HI mass function depends on environment, although the dependence is puzzling. Zwaan et al. (2005) found that the low-mass end of the HI mass function was steeper in higher density environments in their HIPASS data, independent of short-range effects such as galaxy interactions. This would seem counterintuitive, indicating that the number density of galaxies with low HI masses increases as the density of their environment increases, rather than decreasing as would be the case if, say, ram-pressure stripping is efficient.

Doyle & Drinkwater (2006) also investigated the environmental dependence of the HI masses in galaxies, but they focused on the link between HI mass and star formation rate. They concluded that there is a strong correlation between a galaxy's star formation rate and its HI mass, but that star formation rates are relatively insensitive to the local galaxy density, for a given HI mass. Importantly, they found that the number of galaxies with an HI mass above some threshold declines sharply in high density environments, consistent with the well known morphology-density relation.

These observational results suggest that environment plays an important role in determining the HI properties of galaxies. In our next paper we shall explore precisely what role environment is predicted to play in shaping a galaxy's HI properties.

ACKNOWLEDGEMENTS

CP thanks Chris Blake and Lister Staveley-Smith for instructive discussions at various stages during the writing of this paper. This work was supported by separate STFC rolling grants at Leicester and Durham. CP acknowledges the support of the Australian Research Council funded "Commonwealth Cosmology Initiative", DP Grant No. 0665574 during the initial stages of this work. We acknowledge the efforts of Andrew Benson, Richard Bower, Shaun Cole, Carlos Frenk, John Helly and Rowena Malbon in developing the GALFORM code used in the Baugh2005M model. This project was made possible by the availability of models on the Millennium archive set up the Virgo Consortium with the support of the German Astrophysical Virtual Observatory.

REFERENCES

- Abdalla F. B., Blake C. & Rawlings S., 2009, preprint (arXiv:astro-ph/0905.4311)
- Almeida C., Baugh C. M. & Lacey C. G., 2007, MNRAS, 376, 1711
- Almeida C., Baugh C. M., Wake D. A., Lacey C. G., Benson A. J., Bower R. G. & Pimbblet K., 2008, MNRAS, 386, 2145
- Balogh M. L., Navarro J. F. & Morris S. L., 2000, ApJ, 540, 113
- Baugh C. M., 2006, Reports of Progress in Physics, 69, 3101
- Baugh C. M., Lacey C. G., Frenk C. S., Benson A. J., Cole S., Granato G. L., Silva L. & Bressan A., 2004, New Astronomy Review, 48, 1239
- Baugh C. M., Lacey C. G., Frenk C. S., Granato G. L., Silva L., Bressan A., Benson A. J. & Cole S., 2005, MNRAS, 356, 1191
- Benson A. J., Bower R. G., Frenk C. S., Lacey C. G., Baugh C. M. & Cole S., 2003, ApJ, 599, 38
- Benson A. J., Frenk C. S., Baugh C. M., Cole S. & Lacey C. G., 2001, MNRAS, 327, 1041
- Blake C. A., Abdalla F. B., Bridle S. L. & Rawlings S., 2004, New Astronomy Review, 48, 1063

- Bower R. G., Benson A. J., Malbon R., Helly J. C., Frenk C. S., Baugh C. M., Cole S. & Lacey C. G., 2006, *MNRAS*, 370, 645
- Braun R., 2007, preprint (arXiv:astro-ph/0703746)
- Burke B. F. & Graham-Smith F., 1996, *An Introduction to Radio Astronomy*, Cambridge University Press.
- Chengalur J. N., Braun R. & Wieringa M., 2001, *A&A*, 372, 768
- Cole S., Lacey C. G., Baugh C. M. & Frenk C. S., 2000, *MNRAS*, 319, 168
- Cole S. et al., 2001, *MNRAS*, 326, 255
- Croton D. J., Springel V., White S. D. M., De Lucia G., Frenk C. S., Gao L., Jenkins A., Kauffmann G., Navarro J. F. & Yoshida N., 2006, *MNRAS*, 365, 11
- De Lucia G. & Blaizot J., 2007, *MNRAS*, 375, 2
- De Lucia G., Springel V., White S. D. M., Croton D. & Kauffmann G., 2006, *MNRAS*, 366, 499
- Doyle M. T. & Drinkwater M. J., 2006, *MNRAS*, 372, 977
- Drory N., Salvato M., Gabasch A., Bender R., Hopp U., Feulner G. & Pannella M., 2005, *ApJ*, 619, L131
- Font A. S., Bower R. G., McCarthy I. G., Benson A. J., Frenk C. S., Helly J. C., Lacey C. G., Baugh C. M. & Cole S., 2008, *MNRAS*, 389, 1619
- Fontana A. et al., 2004, *A&A*, 424, 23
- Giovanelli R. et al., 2005, *AJ*, 130, 2598
- Gonzalez J. E., Lacey C. G., Baugh C. M., Frenk C. S. & Benson A. J., 2008, preprint (arXiv:astro-ph/0812.4399)
- Gonzalez-Perez V., Baugh C. M., Lacey C. G. & Almeida C., 2008, preprint (arXiv:astro-ph/0811.2134)
- Hopkins A. M., 2004, *ApJ*, 615, 209
- Johnston S. et al., 2008, *Experimental Astronomy*, 22, 151
- Jonas J., 2007, in “From Planets to Dark Energy: the Modern Radio Universe”, October 1-5 2007, The University of Manchester, UK.
- Kennicutt Jr. R. C., 1998, *ApJ*, 498, 541
- Keres D., Yun M. S. & Young J. S., 2003, *ApJ*, 582, 659
- Kitzbichler M. G. & White S. D. M., 2007, *MNRAS*, 376, 2
- Lah P., et al., 2007, *MNRAS*, 376, 1357
- Lah P., Pracy M. B., Chengalur J. N., Briggs F. H., Colless M., De Propriis R., Ferris S., Schmidt B. P. & Tucker B. E., 2009, preprint (arXiv:astro-ph/0907.1416)
- Madau P., Ferguson H. C., Dickinson M. E., Giavalisco M., Steidel C. C. & Fruchter A., 1996, *MNRAS*, 283, 1388
- McCarthy I. G., Frenk C. S., Font A. S., Lacey C. G., Bower R. G., Mitchell N. L., Balogh M. L. & Theuns T., 2008, *MNRAS*, 383, 593
- Meyer M. J. et al., 2004, *MNRAS*, 350, 1195
- Obreschkow D. & Rawlings S., 2009, *MNRAS*, 394, 1857
- Obreschkow D., Croton D., De Lucia G., Khochfar S. & Rawlings S., 2009a, *ApJ*, 698, 1467
- Obreschkow, D., Heywood, I., Klöckner, H. -R., & Rawlings, S., 2009b, preprint (arXiv:astro-ph/0907.3091)
- Parkinson H., Cole S. & Helly J., 2008, *MNRAS*, 383, 557
- Péroux C., McMahon R. G., Storrie-Lombardi L. J. & Irwin M. J., 2003, *MNRAS*, 346, 1103
- Prochaska J. X., Herbert-Fort S. & Wolfe A. M., 2005, *ApJ*, 635, 123
- Quilis V., Moore B. & Bower R., 2000, *Science*, 288, 1617
- Rao S. & Briggs F., 1993, *ApJ*, 419, 515
- Rao S. M., Turnshek D. A. & Nestor D. B., 2006, *ApJ*, 636, 610
- Spitzer L., 1978, *Physical processes in the interstellar medium*, New York Wiley-Interscience.
- Springel V., White S. D. M., Jenkins A., Frenk C. S., Yoshida N., Gao L., Navarro J., Thacker R., Croton D., Helly J., Peacock J. A., Cole S., Thomas P., Couchman H., Evrard A., Colberg J. & Pearce F., 2005, *Nature*, 435, 629
- Verheijen M. A. W., Oosterloo T. A., van Cappellen W. A., Bakker L., Ivashina M. V. & van der Hulst J. M., 2008, in Minchin R., Momjian E., eds, “The Evolution of Galaxies Through the Neutral Hydrogen Window” Vol. 1035 of American Institute of Physics Conference Series.,
- Weinmann S. M., van den Bosch F. C., Yang X. & Mo H. J., 2006a, *MNRAS*, 366, 2
- Weinmann S. M., van den Bosch F. C., Yang X., Mo H. J., Croton D. J. & Moore B., 2006b, *MNRAS*, 372, 1161
- Young J. S. & Scoville N. Z., 1991, *ARA&A*, 29, 581
- Zwaan M. A., 2000, PhD thesis, PhD Thesis, Groningen
- Zwaan M. A., Briggs F. H., Sprayberry D. & Sorar E., 1997, *ApJ*, 490, 173
- Zwaan M. A., Meyer M. J., Staveley-Smith L. & Webster R. L., 2005, *MNRAS*, 359, L30
- Zwaan M. A. et al., 2003, *AJ*, 125, 2842